

Reprinted from *The Journal of Physical Chemistry*, 1991, 95.  
 Copyright © 1991 by the American Chemical Society and reprinted by permission of the copyright owner.

## Time-Dependent Calculation of Thermally Averaged Reaction Rate Constants: Dynamical Displacement Operator Treatment

Nancy Makri<sup>†</sup>

Department of Chemistry, Harvard University, 12 Oxford Street, Cambridge, Massachusetts 02138  
 (Received: April 4, 1991)

The time-dependent operator formulation of the reactive flux-side correlation function [*J. Chem. Phys.* **1991**, *94*, 4949], whose long-time limit yields the quantum mechanical Boltzmann-averaged rate constant, is optimized by including displacement operators in the expansion of the complex time evolution operator. The advantage of this new treatment is that very few terms are needed for the representation of the propagator, thus significantly reducing the numerical effort required in the calculation.

### I. Introduction

Recently, we presented<sup>1</sup> a fully quantum mechanical methodology for calculating finite temperature reaction rate constants. This formulation can be used to study the reaction kinetics of polyatomic systems, provided that the Hamiltonian can be approximately decomposed into a system coupled (strongly) to a bath. Reaction path models<sup>2-5</sup> are known to achieve such a decomposition, and thus the above rate formalism can be applied to reactive molecular collisions. In addition to gas-phase chemistry, this approach is expected to be relevant and useful also in the field of gas–solid interactions; for example, it can be used to study the role of lattice vibrations (phonons) in determining the rates of dissociation and of diffusion of light species, such as hydrogen or deuterium, on surfaces. Application of these ideas to the dynamics of quantum particles (e.g., electrons) in fluids may be possible but is less straightforward.

The calculation is based on the evaluation of a flux correlation function obtained by Miller et al.<sup>6-8</sup> The multidimensional quantum time evolution operator is represented by a mean field form in the space of the bath degrees of freedom, but is constructed to incorporate correlation between the system (i.e., the reaction coordinate) and the bath. This ansatz for the propagator is the operator analogue of the time-dependent self-consistent-field approximation with explicit two-body correlations proposed earlier<sup>9</sup> and leads to *linear* increase in numerical effort with the number of bath degrees of freedom, without significant loss of accuracy. The Boltzmann average is performed by using a mixed coordinate/operator representation of the density matrix,<sup>10,11</sup> which allows the canonical rate constant to be evaluated *directly* from the solution of a set of temperature-dependent coupled first order

differential equations in time with well-behaved initial conditions.

In this paper we present a modified scheme for expanding the complex time evolution operator (i.e., the density matrix) that leads to accelerated convergence with respect to the number of required bath excitation operators. Specifically, we incorporate the system–bath coupling in the zeroth-order term of the expansion via proper displacement operators. This treatment causes the strongest correlation effects to be described by very few terms that correspond to low-order excitation of the bath.

- 
- (1) Makri, N. *J. Chem. Phys.* **1991**, *94*, 4949.
  - (2) Marcus, R. A. *J. Chem. Phys.* **1964**, *41*, 610; **1966**, *45*, 4493, 4500; **1968**, *49*, 2610.
  - (3) Hofacker, G. L. *Z. Naturforsch. A* **1963**, *18*, 607. Fischer, S. F.; Hofacker, G. L.; Seiler, R. *J. Chem. Phys.* **1969**, *51*, 3951.
  - (4) (a) Miller, W. H.; Handy, N. C.; Adams, J. E. *J. Chem. Phys.* **1980**, *72*, 99. Miller, W. H. In *Potential Energy Surfaces and Dynamics Calculations*; Truhlar, D. G., Ed.; Plenum: New York, 1981. Miller, W. H. *J. Chem. Phys.* **1983**, *87*, 3811. Carrington, Jr., T.; Miller, W. H. *J. Chem. Phys.* **1984**, *81*, 3942. Miller, W. H. In *The Theory of Chemical Reaction Dynamics*; Clary, D. C., Ed.; Reidel: Boston, 1986. (b) Miller, W. H.; Ruf, B. A.; Chang, Y. T. *J. Chem. Phys.* **1988**, *89*, 6298. (c) Ruf, B. A.; Miller, W. H. *J. Chem. Soc., Faraday Trans. 2* **1988**, 84.
  - (5) Truhlar, D. G.; Brown, F. B.; Steckler, R.; Isaacson, A. D. In *The Theory of Chemical Reaction Dynamics*; Clary, D. C., Ed.; Reidel: Boston, 1986. Duff, J. W.; Truhlar, D. G. *J. Chem. Phys.* **1975**, *62*, 2477.
  - (6) (a) Miller, W. H. *J. Chem. Phys.* **1974**, *61*, 1823; *Acc. Chem. Res.* **1976**, *9*, 306.
  - (7) Miller, W. H.; Schwartz, S. D.; Tromp, J. W. *J. Chem. Phys.* **1983**, *79*, 4889.
  - (8) For a survey of other methods for calculating flux correlation functions see ref 1.
  - (9) Makri, N. *Chem. Phys. Lett.* **1990**, *169*, 541.
  - (10) Abrikosov, A. A.; Gorkov, L. P.; Dzyaloshinski, I. E. *Methods of Quantum Field Theory in Statistical Physics*; Dover: New York, 1975.
  - (11) (a) Stiles, M. D.; Wilkins, J. W.; Persson, M. *Phys. Rev. B* **1966**, *34*, 4490. (b) Jackson, B. *J. Chem. Phys.* **1986**, *84*, 3535; **1988**, *88*, 1383; **1988**, *89*, 2473.

<sup>†</sup> Harvard Junior Fellow. Present address: School of Chemical Sciences, University of Illinois, Urbana, IL 61801.

In section II we review the time-dependent formalism for the thermal rate constant. Section III introduces displacement operators in the expansion of the (complex time) propagator and derives equations for the new expansion coefficients. The resulting scheme is used to calculate transmission coefficients for the collinear H + H<sub>2</sub> and D + D<sub>2</sub> reactions in the temperature range 200–1000 K; the results of these calculations, which demonstrate the stability, accuracy, and rapid convergence of the present method, are shown in section IV. Finally, a brief discussion is presented in the last section, along with some remarks regarding future application of these ideas.

## II. Time-Dependent Quantum Mechanical Rate Constant Formalism

In this section we review the time-dependent formalism for the quantum mechanical thermal rate constant that was presented in ref 1. We assume that the process of interest can be adequately described by a system–bath Hamiltonian which, for simplicity, we express in the form

$$\hat{H} = \hat{H}_s + \sum_{i=1}^N \hat{H}_i - \sum_{i=1}^N f_i(\hat{s})(\hat{a}_i + \hat{a}_i^\dagger) \quad (2.1)$$

In eq 2.1  $\hat{a}_i^\dagger$  and  $\hat{a}_i$  are raising and lowering operators for the harmonic bath degrees of freedom  $Q_i$  ( $i = 1, \dots, N$ ), which correspond to molecular normal modes and/or lattice phonon vibrations, described by

$$\hat{H}_i = \frac{\hat{P}_i^2}{2m} + \frac{1}{2} m \omega_i^2 \hat{Q}_i^2 = \left( \hat{a}_i^\dagger \hat{a}_i + \frac{1}{2} \right) \hbar \omega_i$$

$$\hat{H}_s = \frac{\hat{p}_s^2}{2m} + V_0(\hat{s})$$

is the Hamiltonian for the “system” (i.e., the reaction coordinate). The coupling functions  $f_i$  can have any form and may depend on the momentum operator  $\hat{p}_s$ . The present rate constant methodology is by no means limited to the above simple form of the Hamiltonian; typically, the Hamiltonian will include additional coupling terms, such as

$$\sum_{i=1}^N g_i(\hat{s})(\hat{a}_i + \hat{a}_i^\dagger)^2$$

which may arise from  $s$ -dependent frequencies (see the example of section IV). In the most general case the bath may not be harmonic; it is still possible and convenient, though, to express the Hamiltonian in a form similar to eq 2.1 by adopting standard second quantized notation for the bath oscillators. Finally, the theory that follows is applicable to cases where different bath oscillators are coupled to one another, provided that these off-diagonal interactions are weak compared to the coupling with the reaction coordinate.

An exact quantum mechanical theory of canonical rate constants, based on the evaluation of reactive flux correlation functions, has been formulated by Yamamoto<sup>12</sup> and by Miller et al.<sup>6,7</sup> According to the work of Miller, Schwartz, and Tromp,<sup>7</sup> the rate constant  $k$  at temperature  $T$  is expressed as the long time limit of the flux–side correlation function  $C_{f,s}(t)$

$$k = Z^{-1} \lim_{t \rightarrow \infty} C_{f,s}(t) \quad (2.2)$$

where  $Z$  is the canonical partition function for the reactants, and the correlation function is defined by the relation

$$C_{f,s}(t) = \text{Tr} \left[ \hat{F} e^{i\hat{H}t/\hbar} / \hbar \hat{h}(\hat{s}) e^{-i\hat{H}t/\hbar} \right] \quad (2.3)$$

Here  $t_c = t - i\hbar\beta/2$  is a complex time that arises from combining the time evolution operator with the Boltzmann operator ( $\beta = 1/k_B T$ ),  $\hat{F}$  is the symmetrized flux operator,

$$\hat{F} = (1/2m)[\hat{p}_s \delta(\hat{s}) + \delta(\hat{s}) \hat{p}_s] \quad (2.4)$$

$h(\hat{s})$  is a step function operator that projects onto the product

region  $s > 0$ , and the “dividing surface” through which the reactive flux is measured is taken for simplicity at  $s = 0$ . Note that the asymptotic value of the flux–side correlation function, and thus the rate constant, is invariant with respect to the location of the dividing surface. (However, this is not true for the short-time behavior of the correlation function.)

Since the eigenstates of the coupled multidimensional Hamiltonian of eq 2.1 are extremely difficult to obtain, the most promising strategy for evaluating the correlation function of eq 2.3 (and thus the rate constant) is via time-dependent methods. This is so because the flux–side correlation function is known<sup>13</sup> to approach its asymptotic value fairly rapidly (within time that is on the order of  $\hbar\beta$  for “direct” reactions). However, there are two problems which must be overcome in order for a time-dependent calculation of thermally averaged time correlation functions to be feasible in practice. First, one must develop accurate and efficient quantum mechanical techniques for following the time evolution of a wave function with the multidimensional system–bath Hamiltonian. And second, a way must be found to perform the thermal averaging over the bath, without having to repeat the tedious dynamical calculation for every single microcanonical (or other equivalent) initial state.

We choose to evaluate the trace in eq 2.3 in the position representation for the reaction coordinate  $s$  and in the eigenstate representation for the vibrational degrees of freedom  $\{Q_i\}$ . By inserting complete sets of position eigenstates for the system coordinate, it is not hard to show that

$$C_{f,s}(t) = \frac{\hbar}{m} \text{Im} \frac{\partial}{\partial s'} \int_0^\infty ds \sum_{\mathbf{n}=0}^\infty \langle \mathbf{n} | \langle s | e^{i\hat{H}t_c/\hbar} | s' \rangle \langle s | e^{-i\hat{H}t_c/\hbar} | 0 \rangle | \mathbf{n} \rangle \Big|_{s'=0} \quad (2.5)$$

Here  $|\mathbf{n}\rangle \equiv \prod_{i=1}^N |n_i\rangle$ , where  $|n_i\rangle$  is an eigenstate of  $\hat{H}_i$  with eigenvalue  $(n_i + 1/2)\hbar\omega_i$ .

The (complex) time evolution operator appears in eq 2.5 in mixed position (for the system) and operator (for the bath) form.<sup>10,11</sup> We introduce the operator  $\hat{U}$ , defined as the  $s$  space position matrix element of the time evolution operator with the time evolution operator for the bath factored out:

$$\langle s | e^{-i\hat{H}t/\hbar} | s_0 \rangle = \hat{U}(s, s_0; t) \exp \left[ -\frac{i}{\hbar} t \sum_{i=1}^N \hat{H}_i \right] \quad (2.6)$$

Use of this definition allows eq 2.5 to be rewritten as

$$C_{f,s}(t) = \frac{\hbar}{m} \prod_{i=1}^N Z_i \text{Im} \frac{\partial}{\partial s'} \int_0^\infty ds \langle \hat{U}(s, s'; t_c) \hat{U}(s, 0; t_c) \rangle_{T, s'=0} \quad (2.7)$$

where  $Z_i$  is the canonical partition function for the  $i$ th oscillator

$$Z_i = \frac{e^{-\hbar\omega_i\beta/2}}{1 - e^{-\hbar\omega_i\beta}}$$

and  $\langle \dots \rangle_T$  denotes Boltzmann averaging.

Finding the exact time evolution of the operator  $\hat{U}$  amounts to solving the general multidimensional quantum dynamical problem, which is (at least at present) impossible in practice, except for short time. We are thus forced to follow the system–bath dynamics approximately. We seek an approximation which should satisfy both of the following criteria:

(i) *Efficiency.* The required numerical effort (i.e., computer time and memory) should not grow very fast as the number of bath degrees of freedom increases. Ideally, we would like the method to scale linearly with the number of bath oscillators. (Recall that the numerical effort for solving the Schrödinger equation exactly grows exponentially with the number of degrees of freedom.)

(ii) *Accuracy.* We would like the approximate dynamics to resemble the exact dynamics as closely as possible during the time period that is relevant in the process of interest. In the particular

(12) Yamamoto, T. *J. Chem. Phys.* **1960**, *33*, 281.

(13) Tromp, J. W.; Miller, W. H. *J. Phys. Chem.* **1986**, *90*, 3482; *Faraday Discuss. Chem. Soc.* **1987**, *84*, 441.

case of the rate constant, this means that the method of approximation should be sufficiently accurate for time long enough for the correlation function of eq 2.3 to reach its asymptotic value.

An approximate scheme for obtaining the quantum dynamics of system–bath problems has been suggested recently,<sup>9</sup> which seems to satisfy both of the above requirements. According to this idea, one includes system–bath correlation explicitly in the wave function, maintaining the mean field form for the interaction among different bath oscillators. Building system–bath correlation into the time-dependent wave function accounts for most of the strong correlation effects, while leaving out correlation among different bath modes makes the calculation practically feasible without significant loss of accuracy. The reason for the latter arises from the special form of the system–bath Hamiltonian; i.e., the physics of the process is described by strong system–bath coupling, which induces strong system–bath correlation in the time-evolved wave function, whereas the absence of direct (or the presence of weak) bath–bath coupling results in the corresponding absence of important correlation between different bath coordinates in the wave function for short or intermediate time. Since obtaining the rate constant via the flux correlation function formalism does not require knowledge of the dynamics for extremely long time, the above approach seems ideally suited here. Generalizing this idea to the time evolution operator rather than a wave function leads<sup>1</sup> to the following ansatz for the evolution of  $\hat{U}$ :

$$\hat{U}(s, s_0; t) = \prod_{i=1}^N \hat{U}_i(s, s_0; t) \quad (2.8)$$

Here each factor  $\hat{U}_i$  is an operator in the space of the  $i$ th degree of freedom. By substituting eq 2.8 in the time-dependent Schrödinger equation and taking mean field type thermal averages with respect to all bath oscillators  $j \neq i$ , one obtains differential equations in time that govern the evolution of each  $\hat{U}_i$ . This procedure leads to the following result

$$i\hbar \dot{\hat{U}}_i = \hat{H}_i^{\text{eff}} \hat{U}_i - \hat{U}_i \hat{H}_i \quad (2.9a)$$

where the effective Hamiltonian for the  $i$ th oscillator is<sup>1</sup>

$$\hat{H}_i^{\text{eff}} = \prod_{j \neq i}^N \langle \hat{U}_j^\dagger \hat{U}_j \rangle_T^{-1} \left( \prod_{j \neq i}^N \hat{U}_j^\dagger \hat{H} \prod_{j \neq i}^N \hat{U}_j \right)_T - i\hbar \sum_{j \neq i} \frac{\langle \hat{U}_j^\dagger \dot{\hat{U}}_j \rangle_T}{\langle \hat{U}_j^\dagger \hat{U}_j \rangle_T} - \sum_{j \neq i} \frac{\langle \hat{U}_j^\dagger \hat{U}_j \hat{H}_j \rangle_T}{\langle \hat{U}_j^\dagger \hat{U}_j \rangle_T} \quad (2.9b)$$

The time-derivative terms on the right-hand side of eq 2.9b correspond to complex  $s$ -dependent “phase” factors, each one of which is arbitrary subject to the constraint that the product of all these factors should have a value determined by the Boltzmann-averaged Schrödinger equation; i.e., the overall  $s$ -dependent “phase” can be partitioned at any given time arbitrarily among the  $N$  bath degrees of freedom. Making a symmetric choice<sup>9</sup> allows each of these terms to be determined from the relation

$$i\hbar \frac{\langle \hat{U}_i^\dagger \dot{\hat{U}}_i \rangle_T}{\langle \hat{U}_i^\dagger \hat{U}_i \rangle_T} = \frac{1}{N} \left[ \frac{\langle \prod_{j=1}^N \hat{U}_j^\dagger \hat{H} \prod_{j=1}^N \hat{U}_j \rangle_T}{\prod_{j=1}^N \langle \hat{U}_j^\dagger \hat{U}_j \rangle_T} - \sum_{j=1}^N \frac{\langle \hat{U}_j^\dagger \hat{U}_j \hat{H}_j \rangle_T}{\langle \hat{U}_j^\dagger \hat{U}_j \rangle_T} \right] \quad (2.10)$$

In order to solve the equations for the operators  $\hat{U}_i$ , each of these operators is expanded in terms of harmonic oscillator excitation operators. The most straightforward expansion scheme is the one adopted in ref 1:

$$\hat{U}_i(s, s_0; t) = \hat{A}_i(s, s_0; t) + \sum_{k=1}^{M_i} \hat{B}_{i,k+}(s, s_0; t) \hat{a}_i^{+k} + \sum_{k=1}^{M_i} \hat{B}_{i,k-}(s, s_0; t) \hat{a}_i^k \quad (2.11)$$

The quantities  $\hat{A}_i$ ,  $\hat{B}_{i,k+}$ , and  $\hat{B}_{i,k-}$  are themselves operators that include (with appropriate coefficients) all powers of the number operator  $\hat{a}_i^\dagger \hat{a}_i$ . Thus, the expansion (2.11) becomes exact in the limit  $M_i \rightarrow \infty$ . By substituting eq 2.11 in eq 2.9, operating on the left with different powers of  $\hat{a}_i$  (or  $\hat{a}_i^\dagger$ ) and taking thermal averages, one obtains the following differential equations for the

thermal averages  $A_i$  and  $B_{i,k+}$  (or  $B_{i,k-}$ ) of the expansion coefficients  $\hat{A}_i$  and  $\hat{B}_{i,k+}$  (or  $\hat{B}_{i,k-}$ ):

$$i\hbar \dot{A}_i = \langle \hat{H}_i^{\text{eff}} \hat{U}_i \rangle_T - \langle \hat{H}_i \rangle_T A_i \quad (2.12a)$$

$$i\hbar \langle \hat{a}_i^k \hat{a}_i^{+k} \rangle_T \dot{B}_{i,k+} = \langle \hat{a}_i^k \hat{H}_i^{\text{eff}} \hat{U}_i \rangle_T - \langle \hat{a}_i^k \hat{a}_i^{+k} \hat{H}_i \rangle_T B_{i,k+} \quad (2.12b)$$

$$i\hbar \langle \hat{a}_i^{+k} \hat{a}_i^k \rangle_T \dot{B}_{i,k-} = \langle \hat{a}_i^{+k} \hat{H}_i^{\text{eff}} \hat{U}_i \rangle_T - \langle \hat{a}_i^{+k} \hat{a}_i^k \hat{H}_i \rangle_T B_{i,k-} \quad (2.12c)$$

Integration of these temperature-dependent differential equations in complex time gives the thermally averaged bath excitation coefficients  $A_i$ ,  $B_{i,k+}$ , and  $B_{i,k-}$  at the “final time”  $t_c$ . The initial conditions are

$$B_{i,k+}(s, s_0; 0) = B_{i,k-}(s, s_0; 0) = 0 \quad (2.13a)$$

and

$$\prod_{i=1}^N A_i(s, s_0; 0) = \langle \hat{U}(s, s_0; 0) \rangle_T = \delta(s - s_0) \quad (2.13b)$$

Numerical integration of equations (2.12) with the singular initial condition given by eq 2.13b would be extremely difficult in purely real time, because  $\langle \hat{U} \rangle_T$  oscillates wildly with constant amplitude at short  $t$ . In the present case, though, where one is interested in the complex time propagator, numerical integration of the above differential equations is stable and fairly straightforward. This is so because the presence of an imaginary time (i.e., temperature) component in  $t_c$  damps the rapid oscillations present in the real time propagator.<sup>14</sup> Thus, in practice, one chooses a sufficiently small but nonzero complex (or purely imaginary) time  $\delta t_c$ , and uses the short-time approximation to the propagator in complex time to construct a well-behaved initial condition for  $\langle \hat{U} \rangle_T$ :

$$\langle \hat{U}(s, s_0; \delta t_c) \rangle_T = \left[ \frac{m}{2\pi i \hbar \delta t_c} \right]^{1/2} \exp \left[ \frac{i}{\hbar} \frac{m}{2\delta t_c} (s - s_0)^2 - \frac{i}{\hbar} \frac{\delta t_c}{2} [V_0(s) + V_0(s_0)] \right] \quad (2.13c)$$

One can then choose the individual  $A_i$  such that their product equals the right-hand side of eq 2.13c; for example,

$$A_i(s, s_0; \delta t_c) = \langle \hat{U}(s, s_0; \delta t_c) \rangle_T^{1/N} \quad (2.13d)$$

Finally, the Boltzmann average that appears in eq 2.7 is expressed in terms of the thermal averages of the expansion operators  $\hat{A}_i$  and  $\hat{B}_{i,k+}$  and  $\hat{B}_{i,k-}$ . This last step, which is necessary in order to proceed, is not exact but introduces small errors that scale as  $1/N$  with the size of the bath. The numerical results presented in section IV, as well as those given in the previous paper, show that the error due to this thermal averaging procedure is small even for a bath of just one degree of freedom. Therefore, we will not be concerned with these errors below, in particular because the present techniques are intended for use primarily in polyatomic problems, where the above finite temperature averaging scheme becomes virtually exact.

We conclude this section by summarizing the above procedure for the calculation of the flux–side correlation function at any given temperature  $T$ . One integrates the temperature-dependent differential equations (2.12), with  $\hat{H}_i^{\text{eff}}$  given from (2.9b), up to final complex time  $t_c = t - i\hbar\beta/2$ . The integration is performed numerically by representing the expansion coefficients on a grid along the  $s$  coordinate. Equations 2.13 determine the initial conditions. This integration is performed twice, once with the initial condition specified by  $s_0 = 0$  (the location of the dividing surface), and once with  $s_0 = s'$ , where  $s'$  is a coordinate point near  $s = 0$  (e.g., the next point on the grid). At the end of the time integration process with each of the two initial conditions the integrand of eq 2.7 is calculated and the integral over  $s$  is computed. Finally, the  $s'$  derivative is evaluated by finite difference, the various multiplicative factors are included, and the imaginary part is taken. Any time integration contour can be chosen; in-

(14) Wahnstrom, G.; Metiu, H. *Chem. Phys. Lett.* 1987, 134, 531.

tegrating along the imaginary time axis first and subsequently along the real axis yields the correlation function as a function of  $t$  directly, from a single calculation. The rate constant is extracted from the long-time limit (plateau region) of the flux-side correlation function.

As demonstrated by the numerical examples of ref 1 and of section IV, the above algorithm is accurate and numerically stable even at low temperature and for long real time. The efficiency gained by this formulation is due to two factors: first, the use of time-dependent boson operator techniques allows calculation of the object of interest directly, without need to diagonalize large Hamiltonian matrices or to represent functions on multidimensional grids; and second, representation of the time-evolution operator by a mean field form in the space of the bath leads to linear increase of the required numerical effort with the number of degrees of freedom involved. Thus, the methodology presented here provides a highly efficient way to obtain thermally averaged reaction rate constants for polyatomic systems by accurate quantum mechanical techniques.

### III. Dynamical Displacement Operators

The central object that is needed in the calculation of the rate constant is the time evolution operator  $\hat{U}$ . In this section we describe an improved scheme for representing this evolution operator, which, as we show in section IV by numerical examples, leads to accelerated convergence.

With the mean field approximation for the interaction among different bath oscillators, eq 2.8, one seeks an efficient scheme of expanding each  $\hat{U}_i$  in terms of  $\hat{a}_i$  and  $\hat{a}_i^\dagger$  (i.e., an expansion form that requires only a few terms). In order to simplify the presentation that follows, we will consider in this section the case of a bath consisting of a single degree of freedom  $Q$ . The two-degree-of-freedom model system-bath Hamiltonian is

$$\hat{H} = \hat{H}_s + \hat{H}_Q - f(\hat{s})(\hat{a} + \hat{a}^\dagger) \quad (3.1)$$

The operator

$$\hat{U}(s, s_0; t) = \langle s | e^{-i\hat{H}t/\hbar} | s_0 \rangle e^{i\hat{H}_Q t/\hbar} \quad (3.2)$$

satisfies the Schrödinger equation,

$$i\hbar \hat{U} = \hat{H}\hat{U} - \hat{U}\hat{H}_Q \quad (3.3)$$

Thus, to generalize the procedure that follows to the case where the bath consists of many oscillators, one solves eq 2.9a (which is the generalization of eq 3.3) for each bath degree of freedom with the (time dependent) effective Hamiltonian given from eq 2.9b.

Typically, the system-bath coupling manifests itself as a continuous change in the minimum energy configuration of the bath along the reaction coordinate. For example, in the case of a process that takes place on the surface of a solid, the coupling reflects the dynamical distortion of the lattice as the reactive particles move away from the transition-state configuration. Consider the function  $\lambda(s)$  that describes the minimum energy configuration of the bath as a function of the reaction coordinate (cf. Figure 1). For the model Hamiltonian of eq 3.1 this function is

$$\lambda(s) = \left[ \frac{2m\omega}{\hbar} \right]^{1/2} \frac{f(s)}{m\omega^2}$$

It is possible to take into account the zeroth-order effect of the coupling by incorporating a displacement operator in the expansion of the time evolution operator  $\hat{U}$ :

$$\hat{U}(s, s_0; t) = \hat{L}(\lambda(s)) \{ \hat{A}(s, s_0; t) + \sum_{k=1}^M \hat{B}_{k+}(s, s_0; t) \hat{a}^{\dagger k} + \sum_{k=1}^M \hat{B}_{k-}(s, s_0; t) \hat{a}^k \} \quad (3.4)$$

[For notational simplicity, we use the same symbols that we used in section II for the expansion coefficients; it should be clear, though, that  $\hat{A}$ ,  $\hat{B}_{k+}$ , and  $\hat{B}_{k-}$  of eq 3.4 are different objects from those of eq 2.11.] In the last equation

$$\hat{L}(\lambda) \equiv e^{-i\hat{p}\lambda/\hbar} \quad (3.5)$$

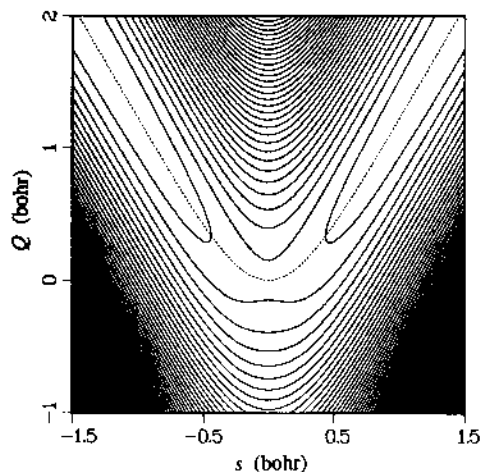


**Figure 1.** Contour plot of the potential in the Cartesian reaction path Hamiltonian model for the collinear H + H<sub>2</sub> reaction with the Porter-Karplus potential surface [see eq 4.2]. The potential contours are spaced by 5 kcal/mol. The dashed line shows the shifting function  $\lambda(s) = Q_0(s)$ .

is a translation operator that shifts any wave function in  $Q$  space by  $\lambda$ :

$$\hat{L}(\lambda) \phi(Q) = \phi(Q - \lambda)$$

By substituting eq 3.4 in eq 3.3, operating from the left by  $\hat{a}^k \hat{L}^\dagger$  (or  $\hat{a}^{\dagger k} \hat{L}$ ),  $k = 0, \dots, N$ , and taking thermal averages, one obtains the following differential equations for the new expansion coefficients:

$$i\hbar \dot{A} = \langle \hat{L}^\dagger \hat{H} \hat{U} \rangle_T - \langle \hat{H}_Q \rangle_T A \quad (3.6a)$$

$$i\hbar \langle \hat{a}^k \hat{a}^{\dagger k} \rangle_T \dot{B}_{k+} = \langle \hat{a}^k \hat{L}^\dagger \hat{H} \hat{U} \rangle_T - \langle \hat{a}^k \hat{L}^\dagger \hat{U} \hat{H}_Q \rangle_T \quad (3.6b)$$

$$i\hbar \langle \hat{a}^{\dagger k} \hat{a}^k \rangle_T \dot{B}_{k-} = \langle \hat{a}^{\dagger k} \hat{L} \hat{H} \hat{U} \rangle_T - \langle \hat{a}^{\dagger k} \hat{L} \hat{U} \hat{H}_Q \rangle_T \quad (3.6c)$$

The averages that appear in eqs 3.6 are straightforward to evaluate. Notice that, since  $\langle \hat{U}(s, s_0; 0) \rangle_T = \delta(s - s_0)$ , the initial conditions for the new coefficients are still given by eqs 2.13, as long as  $\lambda(s_0) = 0$ , which is often satisfied if  $s_0$  is the saddle point of the potential energy surface, since usually  $f(0) = 0$ .

The idea described in the last few paragraphs is reminiscent of a small polaron transformation.<sup>15</sup> It is also similar in spirit to the shifted oscillator basis set suggested previously by Makri and Miller<sup>16</sup> for system-bath problems, and to the quasi-adiabatic basis functions that have been widely used for solving coupled channel scattering equations.<sup>17-23</sup> By incorporating  $s$ -dependent displacement operators in the expansion for  $\hat{U}$ , one forces the evolving wave packet (in wave function rather than operator language) to assume the qualitatively correct shape and to move in the right direction toward the exit channels of the potential, even if no bath excitation operators are included ( $M = 0$ ). We therefore expect this new expansion scheme, eq 3.4, to converge much faster with respect to the number of terms required than the unshifted ( $\lambda = 0$ ) expansion.

### IV. Numerical Application: Rate Constants for the Collinear H + H<sub>2</sub> and D + D<sub>2</sub> Reactions

The collinear H + H<sub>2</sub> reaction

(15) Holstein, T. *Ann. Phys.* **1959**, *8*, 325, 343. (b) Grover, M.; Silbey, R. *J. Chem. Phys.* **1970**, *52*, 2099; **1971**, *54*, 4843. Silbey, R.; Munn, R. W. *J. Chem. Phys.* **1980**, *72*, 2763. Jackson, B.; Silbey, R. *J. Chem. Phys.* **1983**, *78*, 4193.

(16) Makri, N.; Miller, W. H. *J. Chem. Phys.* **1987**, *86*, 1451.

(17) Secrest, D. In *Molecular Collision Theory: A Guide for the Experimentalists*; Bernstein, R. B., Ed.; Plenum: New York, 1979.

(18) Gordon, R. G. *J. Chem. Phys.* **1969**, *51*, 14.

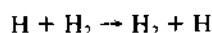
(19) Johnson, B. R. *J. Comput. Phys.* **1973**, *13*, 445.

(20) Light, J. C.; Walker, R. B. *J. Chem. Phys.* **1976**, *65*, 4272. Zvijac, D. J.; Light, J. C. *J. Chem. Phys.* **1976**, *65*, 237. Parker, G. A.; Schmalz, T. G.; Light, J. C. *J. Chem. Phys.* **1980**, *73*, 1757.

(21) Kuppermann, A.; Schatz, G. C.; Baer, M. *J. Chem. Phys.* **1976**, *65*, 4596. Schatz, G. C.; Kuppermann, A. *J. Chem. Phys.* **1976**, *65*, 4642.

(22) Mullaney, N. A.; Truhlar, D. G. *J. Chem. Phys.* **1979**, *71*, 91. Harvey, N. M.; Truhlar, D. G. *J. Chem. Phys. Lett.* **1980**, *74*, 252.

(23) Zhang, J. Z. H.; Miller, W. H. *J. Phys. Chem.* **1990**, *94*, 7785.



constitutes the simplest nontrivial system for testing new theoretical methods in the area of quantum reaction dynamics. The  $\text{H}_3$  system is intrinsically quantum mechanical, with skew angle of  $60^\circ$  which corresponds to significant reaction path curvature. Accurate potential energy surface calculations for this system as well as quantum reactive scattering calculations for the collinear reaction have existed for a long time. Fully converged reactive scattering calculations in three-dimensional space have become possible in recent years.

In ref 1 we applied the methodology described in section II to calculate thermally averaged reaction rate constants for the distinguishable atom version of the collinear  $\text{H} + \text{H}_2$  reaction. These calculations showed that this scheme is numerically stable, efficient, and accurate over a wide temperature range and even when tunneling is very important. However, many (i.e., 10–20) terms had to be included in the expansion of the propagator for the correlation function to converge, particularly so at low temperature. Here we demonstrate the rapid convergence that can be accomplished if the modified scheme of section III, eq 3.4, is adopted in the expansion of the time evolution operator. We use the Porter–Karplus potential surface<sup>24</sup> and report rate constant calculations for the collinear  $\text{H} + \text{H}_2$  system, as well as for its isotopic equivalent, the  $\text{D} + \text{D}_2$  reaction, in the temperature range 200–1000 K. In order to bring the Hamiltonian in the desirable system–bath form, we adopt again a Cartesian reaction path model.<sup>4c</sup> The specific form of the Hamiltonian is<sup>25</sup>

$$\hat{H} = \frac{\hat{p}_s^2}{2m} + \frac{\hat{p}^2}{2m} + V_0(s) + \frac{1}{2}V_2(s)[Q - Q_0(s)]^2 \quad (4.1)$$

In the last equation  $m$  is the reduced mass of the system,  $m = 2/3m_{\text{H}}$  (or  $m = 2/3m_{\text{D}}$ ) and  $\omega = (V_2(0)/m)^{1/2}$  is the frequency at the transition state. The potential  $V_0$  has the shape of a barrier. At large  $s$  the function  $V_2$  approaches a constant, while  $Q_0(s) \propto |s|$ . A contour plot of this potential is shown in Figure 1.

The Hamiltonian is brought in system–bath form by writing

$$\hat{H} = \hat{H}_s + \hat{H}_Q - f(s)(\hat{a} + \hat{a}^\dagger) + g(s)(\hat{a} + \hat{a}^\dagger)^2 \quad (4.2)$$

where

$$\hat{H}_s = \frac{\hat{p}_s^2}{2m} + V_0(s) + \frac{1}{2}V_2(s) Q_0(s)^2 \quad (4.3a)$$

is the Hamiltonian for the reaction coordinate  $s$

$$\hat{H}_Q = \frac{\hat{p}^2}{2m} + \frac{1}{2}m\omega^2 Q^2 \quad (4.3b)$$

describes the bath, and the coupling functions are

$$f(s) = \left[ \frac{\hbar}{2m\omega} \right]^{1/2} V_2(s) Q_0(s) \quad (4.3c)$$

$$g(s) = \frac{\hbar}{2m\omega} \frac{1}{2} [V_2(s) - m\omega^2] \quad (4.3d)$$

This Hamiltonian is an example where the coupling is *not* purely linear in the bath coordinate  $Q$ . The shifting function was chosen as the value of  $Q$  for which the potential energy at each value of the reaction coordinate is minimum:

$$\lambda(s) = Q_0(s)$$

This function is depicted in Figure 1 by the dashed line on the contour plot of the potential.

The calculation of the rate constant was performed for  $T = 200, 300, 600,$  and  $1000$  K. The flux–side correlation function, eq 2.3, was computed at each temperature using the time-dependent methodology of section II, with the displacement operator

TABLE I: Quantum Correction Factor  $\kappa$  for the Collinear  $\text{H} + \text{H}_2$  Reaction

$T, \text{K}$	$M = 0$	$M = 1$	$M = 2$	$M = 3$	$M \rightarrow \infty$	basis set <sup>a</sup>
1000	1.16	1.52	1.54	1.55	1.5	1.5
600	1.45	2.14	2.26	2.37	2.4	2.5
300	3.19	6.08	7.12	8.06	8.4	8.7
200	10.9	21.0	32.7	39.5	43	46

<sup>a</sup> Reference 25.

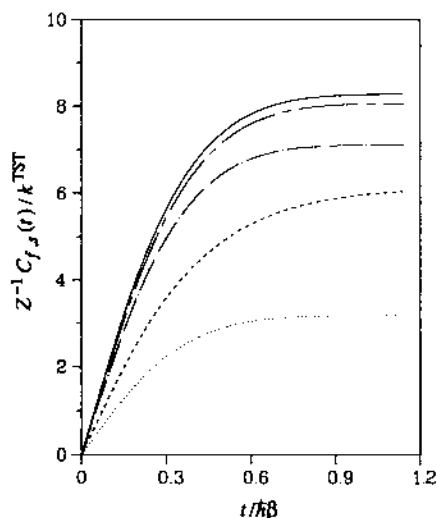


Figure 2. The flux–side correlation function  $C_{fs}(t)$  (divided by the partition function  $Z$  and by the transition-state-theory rate constant), as a function of time for the collinear  $\text{H} + \text{H}_2$  reaction at  $T = 300$  K as obtained with the shifted operator scheme of section III. Dotted line,  $M = 0$ ; dashed line,  $M = 1$ ; chain-dotted line,  $M = 2$ ; chain-dashed line,  $M = 3$ ; solid line,  $M = 4$ .

representation of the complex time propagator described in section III. The coupled differential equations for the expansion coefficients were integrated first in pure imaginary time up to the value  $-i\hbar\beta/2$ , and subsequently in real time  $t$ , to give  $C_{fs}(t)$ . The plateau region of  $C_{fs}(t)$  determines the rate constant according to eq 2.2.

For every temperature considered, the correction factor  $\kappa$  to the transition state theory<sup>26–28</sup> rate was calculated. The quantum correction factor (or transmission coefficient) is defined as the ratio of the quantum mechanical rate constant divided by the transition-state theory rate:

$$\kappa = k^{\text{QM}} / k^{\text{TST}} \quad (4.4)$$

The results are shown in Tables I and II as a function of  $M$ , the number of off-diagonal bath states included in the expansion of  $\hat{U}$  [cf. eq 3.4].

Table I shows the quantum correction factor  $\kappa$  for the  $\text{H} + \text{H}_2$  reaction vs  $M$  at  $T = 1000, 600, 300,$  and  $200$  K. Tunneling effects are very significant at low temperature for this system, and transition-state theory is seen to underestimate the rate by a factor  $>40$  at  $200$  K. Examination of the results shown in Table I as a function of  $M$  shows the rapid convergence achieved by the present scheme; namely, exact results are obtained by including a single bath excitation operator at  $1000$  K. More raising and lowering operators are necessary to obtain accurate results at lower temperature, but it is encouraging that the converged ( $M \rightarrow \infty$ ) results are approached very fast. For example, error smaller than 30% is achieved with  $M = 0, 1, 1,$  and  $2$  for  $T = 1000, 600, 300,$  and  $200$  K, respectively. It is perhaps worth emphasizing that

(26) Glasstone, S.; Laidler, K. J.; Eyring, H. *The Theory of Rate Processes*; McGraw-Hill: New York, 1941.

(27) Pechukas, P. In *Dynamics of Molecular Collisions*; Miller, W. H., Ed.; Plenum: New York, 1976. Pechukas, P. *Annu. Rev. Phys. Chem.* **1981**, *32*, 159.

(28) (a) Truhlar, D. G.; Kuppermann, A. *J. Am. Chem. Soc.* **1971**, *93*, 1840; *Chem. Phys. Lett.* **1971**, *9*, 269; *J. Chem. Phys.* **1972**, *56*, 2232. (b) Garrett, B. C.; Truhlar, D. G. *Proc. Natl. Acad. Sci. U.S.A.* **1979**, *76*, 4755. (c) Truhlar, D. G.; Hase, W. L.; Hynes, J. T. *J. Phys. Chem.* **1983**, *87*, 2664.

(24) Porter, R. N.; Karplus, M. *J. Chem. Phys.* **1964**, *40*, 1105.

(25) Tromp, J. W. Ph.D. Thesis, Lawrence Berkeley Laboratory, University of California, 1988.

**TABLE II: Quantum Correction Factor  $\kappa$  for the Collinear D + D<sub>2</sub> Reaction**

$T, K$	$M = 0$	$M = 1$	$M = 2$	$M = 3$	$M \rightarrow \infty$
1000	1.13	1.36	1.38	1.39	1.4
600	1.40	1.84	1.91	1.94	2.0
300	3.16	5.02	5.45	5.73	5.9
200	11.7	18.8	22.9	25.6	27

the value of  $M$  necessary for convergence corresponds to the number of states *off-diagonally coupled* to each zeroth-order state of the bath, and is *not* related to the number of bath states that are populated at the given temperature; the latter increases with increasing temperature, while the required number of bath excitation operators decreases with  $T$ .

Figure 2 shows the flux-side correlation function  $C_{fs}(t)$  for the collinear H + H<sub>2</sub> reaction at 300 K for  $M = 0, 1, 2, 3$ , and 4, as a function of the real time  $t$ . The corresponding expansion coefficients  $A(s,0;t_c)$  and  $B_{k+}(s,0;t_c)$ ,  $k = 1, \dots, M$  at  $t_c = t - i\hbar\beta/2$  are shown (for  $M = 0, 1, 2$ , and 3) in Figure 3. Recall that these functions are related to Boltzmann averages of the complex time propagator  $\hat{U}$ , i.e.,  $A(s,0;t_c) = \langle \hat{L}^\dagger \hat{U}(s,0;t_c) \rangle_T$ , etc.

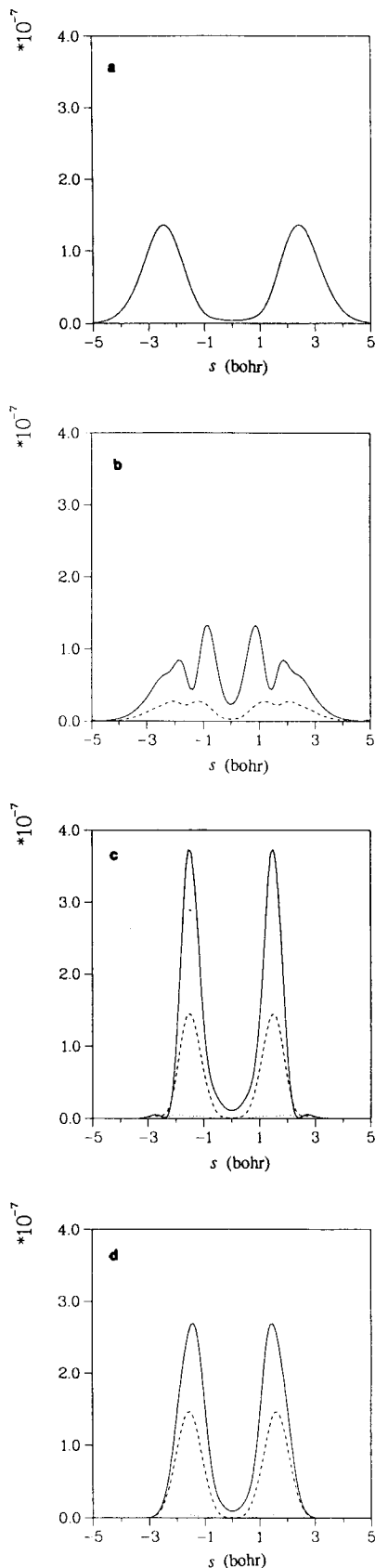
Finally, Table I shows results of accurate basis set calculations available<sup>25</sup> for the H + H<sub>2</sub> system with the Porter-Karplus potential surface. It is seen that the converged rate constant results obtained with the present methodology are in very good agreement with the exact results. Small errors of the present scheme are due to the system-bath approximation for the potential, as well as to the thermal averaging procedure (see the discussion in section II and in ref 1).

Table II shows similar results for the D + D<sub>2</sub> reaction. The reduced mass for that system is larger by a factor of 2 compared to that for H + H<sub>2</sub>, and thus the tunneling correction to transition-state theory is smaller. To the author's knowledge, basis set results are not available for the collinear D + D<sub>2</sub> reaction with the Porter-Karplus potential surface, but the convergence rate of the present time-dependent approach as  $M$  is increased is even faster than in the case of hydrogen; for example, less than 30% error is achieved with  $M = 1$ , even at the lowest temperature considered here.

## V. Discussion

The time-dependent evaluation of Miller's flux-side correlation function presented in ref 1 and in section II of this paper provides an accurate, numerically stable, and highly efficient method for calculating quantum mechanical Boltzmann-averaged reaction rate constants. The mixed position-operator representation of the time evolution operator allows the thermal average with respect to the bath degrees of freedom to be performed analytically, thus circumventing the need to construct and propagate high-dimensional density matrices. A mean field ansatz for the propagator in the space of the bath is used, while the system-bath interaction is treated in a fully correlated fashion. As a consequence of this mean field approach that includes system-bath correlation, the numerical effort for the calculation of the rate constant grows linearly with the number of bath degrees of freedom involved, and yet the system-bath dynamics is treated accurately. The use of dynamical displacement operators in the expansion of the time evolution operator described in section III of this paper further reduces the number of equations to be solved, as it takes into account the system-bath coupling in the zeroth-order part of the expansion. The results of test calculations reported in section IV show that this new expansion scheme requires very few terms to converge, such that even *exact* calculations (i.e., without the mean field treatment for the bath) can probably be performed this way for several interesting bimolecular reactions in three spatial dimensions.

For the above methodology to find more general use, several questions which we did not attempt to answer in this paper must be considered. Perhaps the most important question is the ability of reaction path models to describe more complicated reactive processes in the gas phase or in the condensed phase. Certain "heavy-light-heavy" situations may present a challenge, both to



**Figure 3.** Absolute square of the thermally averaged complex time propagator expansion coefficients  $A(s,0;t_c) \equiv \langle \hat{L}^\dagger \hat{U}(s,0;t_c) \rangle_T$  (solid line) and  $B_{k+}(s,0;t_c) \equiv \langle \hat{L}^\dagger \hat{a}^k \hat{U}(s,0;t_c) \rangle_T$ ,  $k = 1, \dots, M$  (dashed and dotted lines) as a function of the reaction coordinate  $s$  at  $t \approx \hbar\beta$  for the same system at  $T = 300$  K. (a)  $M = 0$ . (b)  $M = 1$ . (c)  $M = 2$ . (d)  $M = 3$ .

the validity of the reaction path approximation and to the efficiency of the present displacement operator scheme. Finally, the feasibility and accuracy of the time-dependent self-consistent-field

approximation with two-body correlations has so far been tested only for the propagation of wave functions in model system-bath Hamiltonians.<sup>9</sup> These models used realistic potentials with barriers very similar to those encountered in H-exchange reactions, and the test calculations showed the mean field approximation with explicit system-bath correlation to be extremely accurate over times long enough for the wave packet to move away from the saddle point region. Nevertheless, numerical calculations of rate constants for problems with three or more degrees of freedom must

be carried out to verify the applicability of the approach presented here to more challenging problems. Some such applications are in progress.

*Acknowledgment.* This work has been supported by a Junior Fellowship from the Society of Fellows, Harvard University. The calculations reported were performed on a SUN 4/65 SPARC 1 station, funded by the Milton Fund Award of the Harvard Medical School.